

# Analytical and experimental studies on the diode-pumped, simultaneously Q-switched and mode-locked *c*-cut Nd:GdVO<sub>4</sub>/KTP green laser with LT-GaAs absorber

M. Li<sup>a</sup>, S. Zhao, G.Q. Li, K. Yang, D. Li, J. Wang, and J. An

School of Information Science and Engineering, Shandong University, Jinan 250100, P.R. China

Received 4 December 2006

Published online 30 March 2007 – © EDP Sciences, Società Italiana di Fisica, Springer-Verlag 2007

**Abstract.** A diode-pumped passively Q-switched mode-locked (QML) intracavity frequency doubled *c*-cut Nd:GdVO<sub>4</sub>/KTP green laser with a LT-GaAs saturable absorber is presented. More than 90% modulation depth for the mode-locked green pulses has been achieved. Using the hyperbolic secant function methods, a developed rate equation model for Q-switched and mode-locked lasers considering the Gaussian spatial distribution of the intracavity photon intensity, the influences of continuous pump rate, the upper state lifetime of the active medium, and the excited-state lifetime of the saturable absorber, was proposed. With this developed model, the theoretical results are in good agreement with the experimental results and the width of the mode-locked green pulse was estimated to be about 380 ps.

**PACS.** 42.60.Fc Modulation, tuning, and mode locking – 42.60.Gd Q-switching – 42.55.Xi Diode-pumped lasers

## 1 Introduction

Laser sources at 532 nm with high repetition rate, high peak power and moderate average power have attracted great attention in the recent years [1–3] and are widely used in many medical applications including surgery, angioplasty and dermatology, as well as in other fields of science and technology such as information storage, coherent telecommunications etc. Using simultaneous passive Q-switching and mode-locking in a diode-pumped intracavity frequency-doubled Nd-doped laser operating at 1.06  $\mu\text{m}$  fundamental wavelength, such sources can be easily realized and have the advantages of simplicity, compactness, low cost and high efficiency. So far, a variety of saturable absorbers for Q-switching and mode-locking (QML) have been investigated, such as LiF:F<sub>2</sub> [4], Cr<sup>4+</sup>:YAG crystals [5–7], GaAs wafer [8–13], and semiconductor saturable absorption mirrors [14–16], and so on. Among these saturable absorbers, GaAs wafer has been widely used for passively Q-switched and mode-locked 1  $\mu\text{m}$  lasers, especially for the Nd<sup>3+</sup> doped materials working at 1.06  $\mu\text{m}$  for its virtues of cheap and easy fabrication as well as high damage threshold. However, its modulation depth is limited and cannot be modulated [17]. An efficient method to improve the modulation depth of GaAs is to use a low temperature GaAs (LT-GaAs) saturable absorber. In LT-GaAs absorber, when As fluence is excessive over Ga fluence, antisites (or As<sub>Ga</sub>) and Ga vacancy

(or V<sub>Ga</sub>) will be generated, which can form the trapping energy levels similar to EL2 defect in semi-insulated GaAs wafer [10]. So the only difference between the defect energy level in LT-GaAs and the EL2 level in GaAs is that the defect density in LT-GaAs is much more than that of the EL2 level in GaAs wafer. Therefore, the modulation of LT-GaAs absorber can reach tens of hundredth if only the LT-GaAs is thick enough. The modulation depth can also be increased by decreasing the temperature of the GaAs absorption layer and the recovery time decreases with the temperature for growth. That is to say, the parameters for Lt-GaAs absorber are adjustable. Although the principle for LT-GaAs as an absorber for mode locking is not very clear, it is believed that single photon absorption (SPA) involved with EL2 defects, two photon absorption (TPA) between conduction and valence band and free-carrier absorption (FCA) effects play an important role.

Nd:GdVO<sub>4</sub>, as a novel isomorph of Nd:YVO<sub>4</sub>, has been confirmed to be a promising laser medium for diode pumping [10–12]. Especially, because of its broader gain bandwidth and higher thermal conductivity, Nd:GdVO<sub>4</sub> crystal is more competent than Nd:YVO<sub>4</sub> when operated in mode-locking state. The conventional *a*-cut Nd:GdVO<sub>4</sub> crystal has large stimulated emission cross section and lower threshold power in comparison with *c*-cut Nd:GdVO<sub>4</sub>, but the *c*-cut Nd:GdVO<sub>4</sub> laser has a higher slope efficiency because the intrinsic loss of *c*-cut Nd:GdVO<sub>4</sub> crystal is smaller than the *a*-cut one [13]. Very recently, a simultaneously passively Q-switched and

<sup>a</sup> e-mail: dabaojiu@126.com

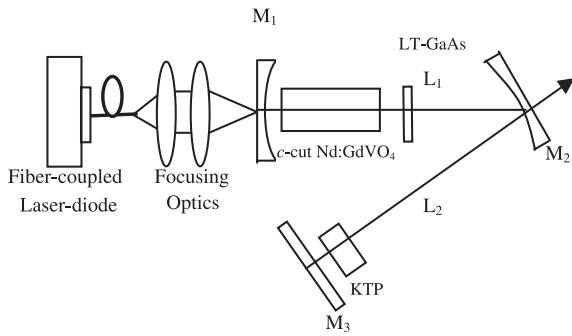


**Fig. 1.** Schematics for passively Q-switched and mode-locked *c*-cut Nd:GdVO<sub>4</sub>/KTP green laser.

mode-locked *c*-cut Nd:GdVO<sub>4</sub> laser at 1.06  $\mu\text{m}$  with Cr<sup>4+</sup>:YAG saturable absorber has been realized [10]. As compared with Q-switched and mode-locked *a*-cut Nd:GdVO<sub>4</sub> laser, the *c*-cut Nd:GdVO<sub>4</sub> laser has a lower repetition rate and higher pulse peak power of the Q-switched envelop. All the features implies the excellent laser performance of the *c*-cut Nd:GdVO<sub>4</sub> crystals for high-peak-power Q-switched and QML operation. However, there hasn't been any report on the QML operation at 0.53  $\mu\text{m}$  using *c*-cut Nd:GdVO<sub>4</sub> crystal as the gain medium with LT-GaAs.

In this paper, for the first time as far as we know, we demonstrated a diode-pumped passively Q-switched and mode-locked *c*-cut Nd:GdVO<sub>4</sub>/KTP green laser with LT-GaAs wafer simultaneously as the saturable absorber in a V-type folded cavity. Using the hyperbolic secant function methods, we have introduced a rate equation mode for the Q-switched and mode-locked *c*-cut Nd:GdVO<sub>4</sub>/KTP green laser, in which not only the Gaussian distribution of the intracavity photon lifetime of the active medium and the excited-state lifetime of the saturable absorber were taken into account. With this model, the theoretical evaluations are in good agreement with the experiments.

## 2 Experimental setup and results

The schematic of our experimental setup is shown in Figure 1. A V-type folded cavity is designed to allow mode matching with the pump beam and to provide the small spot sizes in the pump beam and the saturable absorber. The pump source is a fiber-coupled laser-diode (FAP system, COHERENT Inc., USA) which works at the maximum absorption wavelength (808 nm) of the Nd<sup>3+</sup> ions. A 1.0-at.% Nd<sup>3+</sup>, 4 × 4 × 5 mm<sup>3</sup> *c*-cut Nd<sup>3+</sup>:GdVO<sub>4</sub> crystal is used as the laser active material. One surface of the crystal is coated high transmission (HT) at 808 nm, whereas the other surface of the crystal is anti-reflection (AR) at 1064 nm. The KTP crystal cut for type-II phase matching is 3 × 3 × 8 mm<sup>3</sup> and both of its surfaces are antireflection coated at 1064 nm and 532 nm. The temperatures of the *c*-cut Nd<sup>3+</sup>:GdVO<sub>4</sub> crystal and the KTP crystal are controlled at 20 °C and 22 °C by using semiconductor cooler, respectively. The input mirror M<sub>1</sub> is a concave with 150 mm curvature radius, with HT at 808 nm and high

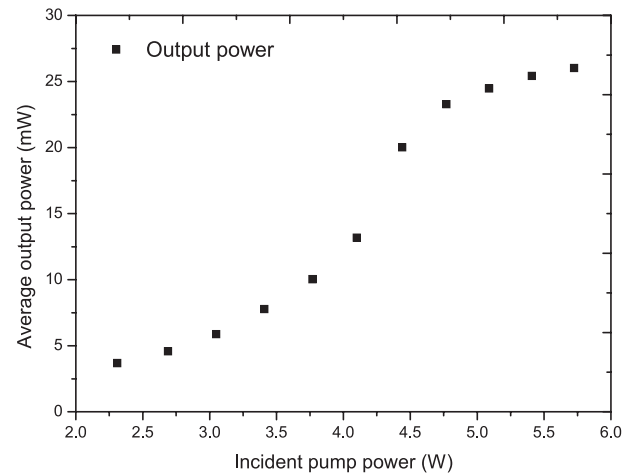


**Fig. 2.** Dependence of the average output power of the Q-switched green pulse train on the incident pump power in the QML Nd:GdVO<sub>4</sub> laser.

reflection (HR) at 1064 nm. The curvature radius of the folded mirror M<sub>2</sub> is 500 mm with anti-transmission (AT) at 1064 nm. The output mirror M<sub>3</sub> is flat mirror with AT at both 1064 nm and 532 nm. The length between M<sub>1</sub> and M<sub>2</sub> was about 60 cm and the length between M<sub>2</sub> and M<sub>3</sub> was about 46 cm. In this arrangement, the whole cavity length adds up to 106 cm.

The LT-GaAs absorber is used as the saturable absorbers in the experiment. The LT-GaAs absorber was grown using a metal organic vapor phase epitaxy device following the steps: first, a 500 nm GaAs buffer layer was deposited on the semi-insulating GaAs substrate; second, a GaAs layer approximately 3  $\mu\text{m}$  was grown on the buffer layer at a temperature of as low as 550 °C; third, the back of the GaAs substrate was polished and five pairs of SiO<sub>2</sub> and Al<sub>2</sub>O<sub>3</sub> layers were antireflection coated on the LT-GaAs layer; Finally, the other side of the GaAs substrate was antireflection coated with five pairs of SiO<sub>2</sub> and Al<sub>2</sub>O<sub>3</sub> layers.

The temporal shape of the output laser pulse is recorded with a digital oscilloscope (TED620B, 500-MHz bandwidth and 2.5 Gs/s sampling rate, Tektronix Inc., USA) and a fast Si PIN photodiode with a rise time of about 1ns. A MAX 500AD laser power meter (COHERENT Inc., USA) is used to measure the generated average output power.

Figure 2 shows the average output power of the Q-switched pulse train versus the incident pump power. The threshold of the Q-switched pulse train is about 1.60 W, but just when the incident pump power reaches 2.31 W, we can get the Q-switched and mode-locked pulse. The output power increases with increasing incident pump power and the maximum average output power of 26.22 mW is obtained at the incident pump power of 5.72 W. The dependence of the repetition rate of Q-switched pulses on the incident pump power is shown in Figure 3. The repetition rate increase from 45 to 92 kHz when the incident pump power increase from 2.31 to 5.72 W. According to the average output power and the repetition rate, the pulse energy

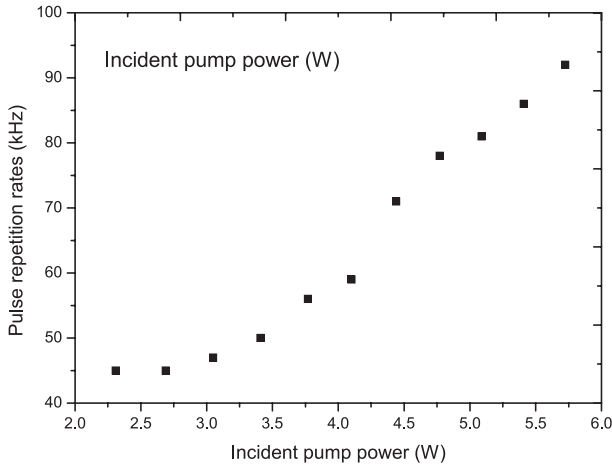


**Fig. 3.** Dependence of the repetition rates of the Q-switched green pulse train on the incident pump power in the QML Nd:GdVO<sub>4</sub> laser.

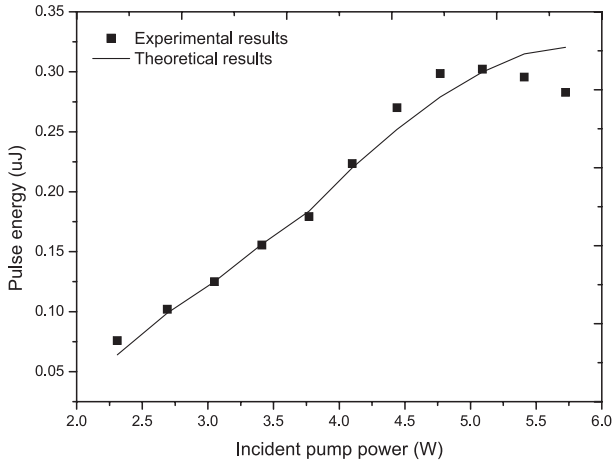


**Fig. 4.** Theoretical and experimental dependence of the pulse energy of the Q-switched green pulse on the incident pump power.

of the second-harmonic (SH) Q-switched pulse versus the incident power is experimentally shown as dots in Figure 4. The single pulse energy increases from 0.076 to 0.3022  $\mu\text{J}$  with the incident pump power increase from 2.31 to 5.05 W. As the average output power increases more slowly than the repetition rate, when the incident pump power increases from 5.05 W, the energy of single Q-switched pulse decrease. The thermal effects may be playing a role. Figure 5 shows the temporal shape of a single passively Q-switched green pulse envelope, which was recorded at the pump power of 4.8 W. The more than 90% modulation depth of the Q-switched mode-locked green pulses could be achieved at any pump power over 2.31 W. The mode-locked pulse interval with the Q-switched envelope is about 640 ns. The expanded oscilloscope traces of a train of mode-locked pulses are showed in Figure 6, from which we obtain that the mode-locked pulses within the Q-switched envelope are separated by 7.0 ns, which matches exactly with the cavity roundtrip transmit time

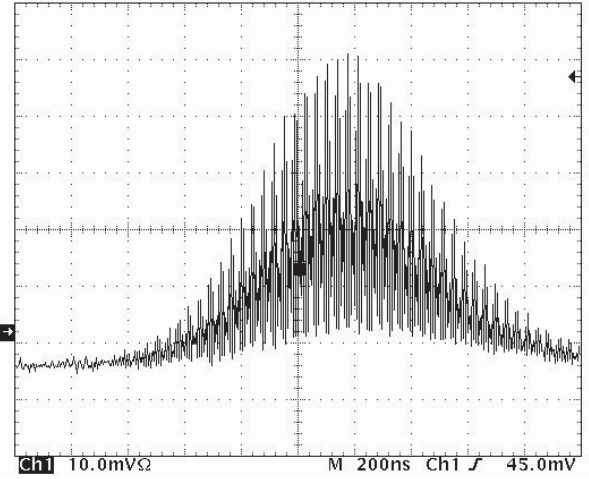


**Fig. 5.** Oscilloscope traces of a typical Q-switched and mode-locked green laser pulse envelope at the incident pump power of 4.8 W.

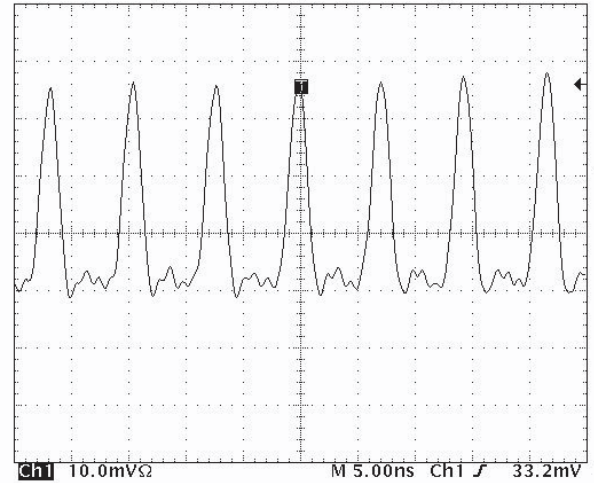


**Fig. 6.** Expanded oscilloscope traces of a train of mode-locked green pulses.

and corresponds to a repetition rate of 143 MHz. With a close observation, the average rise time of the mode-locked pulse is found to be about 1.28 ns. The formula

$$t_{measure} = \sqrt{t_{real}^2 + t_{probe}^2 + t_{oscilloscope}^2}$$

describes the relationships among the measured rise time  $t_{measure}$ , the real rise time  $t_{real}$  of the pulse, the rise time  $t_{probe} = 1$  ns of the probe and  $t_{oscilloscope}$  of the oscilloscope employed. The rise time of oscilloscope  $t_{oscilloscope}$  is determined by  $t_{oscilloscope} \times BW = 0.35-0.4$ , where  $BW = 500$  MHz is the bandwidth of the oscilloscope, so we can get the value of  $t_{oscilloscope}$  is 0.7–0.8 ns. The SH mode-locked pulse width is approximately equal to the real rising time, and from the above-mentioned equation we can obtain the value of 380 ps.

**Table 1.** The parameters of the theoretical calculation [22–24].

Parameters	Values	Parameters	Values
$\sigma$	$1.2 \times 10^{-19} \text{ cm}^2$	$n_{e2}^{2\omega}$	1.79
$\sigma^0$	$1.0 \times 10^{-16} \text{ cm}^2$	$n_{e2}^\omega$	1.746
$\sigma^+$	$2.3 \times 10^{-17} \text{ cm}^2$	$n_{e1}^\omega$	1.83
$\tau$	90 $\mu\text{s}$	$l$	0.5 cm
$n_1$	2.19	$l_s$	580 $\mu\text{m}$
$n_2$	1.83	$d$	1.0 cm
$n_3$	3.48	$d_{\text{eff}}$	7.2 pm/v
$L_p$	106 cm	$L$	0.05
$\omega_p$	250 $\mu\text{m}$	$\varepsilon_0$	$8.855 \times 10^{-12} \text{ C}^2/\text{N m}^2$
$\omega_0$	220 $\mu\text{m}$	$R$	0.995
$\omega_K$	138 $\mu\text{m}$	$\beta$	$2.6 \times 10^{-8} \text{ cm W}^{-1}$
$\omega_G$	140 $\mu\text{m}$		

### 3 Theoretical analysis and discussion

#### 3.1 Theory of fluctuation mechanism and rate equations

The fluctuation mechanism has been proposed to explain the generation of picosecond pulses in simultaneously Q-switched and mode-locked lasers with saturable absorbers [18]. In reference [19], a rate equation model based on the plane wave approximation has been introduced. In this paper, we presented a developed rate equation model, in this model we considered the Gaussian spatial distribution of the intracavity photon intensity by introducing the coefficient of the Gaussian spatial distribution  $\exp(-2r^2/w_l^2)$  in this model. The average photon intensity shape can be described as [7, 19, 20]:

$$\phi(r, t) = \sum_{k=0}^{\infty} \Phi_k f(t - t_k) \exp\left(-\frac{2r^2}{w_l^2}\right) = \phi(0, t) \exp\left(-\frac{2r^2}{w_l^2}\right) \quad (1)$$

where  $\phi(0, t) = \sum_{k=0}^{\infty} \Phi_k f(t - t_k)$ ,  $t_k = kt_r$ ,  $\Phi_k$  is the relative amplitude of the mode-locked pulses at the  $k$ th round trip,  $t_r = 2[n_1l + n_2l_A + n_3d + (L_c - l - l_A - d)]/c$  is the cavity round-trip time,  $n_1$ ,  $n_2$  and  $n_3$  are the refractive indices of the gain medium, LT-GaAs wafer and KTP, respectively,  $l$ ,  $l_A$  and  $d$  are the lengths of the gain medium, LT-GaAs wafer and KTP, respectively,  $L_c$  is the physical length of the cavity,  $c$  is the light velocity;  $w_l$  is the average radius of TEM<sub>00</sub> mode oscillating in the cavity;  $f(t)$  is the mode-locked pulse evolving from the noise and satisfies  $\int_{-\infty}^{\infty} c\sigma f(t) dt = 1$ . If  $f(t)$  is a hyperbolic secant function, it can be written as [2]:

$$f(t) = \frac{1}{2\sigma c\tau_p} \text{sech}^2(t/\tau_p) \quad (2)$$

where  $\sigma$  is the stimulated emission cross section of the gain medium,  $\tau_p$  is related to the FWHM mode-locked pulse duration  $\tau$  at fundamental wavelength by  $\tau = 1.76\tau_p$ .

So the temporal Gaussian shape of the average photon intensity for the pulse at the  $k$ th round trip can be described as:

$$\phi_k(r, t) = \Phi_k f(t) \exp(-2r^2/w_l^2). \quad (3)$$

Using the rate equations method as can be seen in reference [20], in which the Gaussian spatial distribution of the intracavity photon intensity, the influences of continuous pump rate, the upper state lifetime of the active medium, and the excited-state lifetime of the saturable absorber are considered, we can obtain the recurrence relation of the relative amplitude for diode-pumped simultaneously Q-switched and mode-locked  $c$ -cut Nd:GdVO<sub>4</sub>/KTP laser with LT-GaAs wafer:

$$\begin{aligned} \Phi_k = \Phi_{k-1} \exp \left\{ \frac{2}{\pi w_l^2} \int_0^\infty \left[ 2\sigma n(r, t_k) l \frac{w_l^2}{w_G^2} \exp\left(-\frac{2r^2}{w_G^2}\right) \right. \right. \\ \left. \left. - 2\sigma^+ n^+(r, t_k) l_A \frac{w_l^2}{w_A^2} \exp\left(-\frac{2r^2}{w_A^2}\right) \right. \right. \\ \left. \left. - 2\sigma^0 [n_0 - n^+(r, t_k)] l_A \frac{w_l^2}{w_A^2} \exp\left(-\frac{2r^2}{w_A^2}\right) \right. \right. \\ \left. \left. - Bl_A \frac{w_l^4}{w_A^4} \exp\left(-\frac{4r^2}{w_A^2}\right) \Phi_k - \delta_k \frac{w_l^4}{w_{ktp}^4} \exp\left(-\frac{4r^2}{w_{ktp}^2}\right) \Phi_k \right. \right. \\ \left. \left. - \left[ L + \ln\left(\frac{1}{R}\right) \right] \exp\left(-\frac{2r^2}{w_l^2}\right) \right] 2\pi r dr \right\} \quad (4) \end{aligned}$$

$$\begin{aligned} n(r, t_k) = \exp\left(-\frac{t_k}{\tau}\right) \prod_{m=0}^{k-1} \exp\left[-\frac{w_l^2}{w_G^2} \exp\left(-\frac{2r^2}{w_G^2}\right) \Phi_m\right] \\ \times \left\{ R_{in}(r) \exp\left(\frac{t_k}{\tau_a}\right) \int_0^{t_k} \prod_{m=0}^{k-1} \exp\left[\frac{w_l^2}{w_G^2} \exp\left(-\frac{2r^2}{w_G^2}\right) \Phi_m\right] dt \right. \\ \left. + n_i \exp\left(-\frac{2r^2}{w_p^2}\right) \right\} \quad (5) \end{aligned}$$

$$\begin{aligned} n^+(r, t_k) = \left[ \prod_{m=0}^{k-1} \exp\left[-\frac{w_l^2}{w_A^2} \exp\left(-\frac{2r^2}{w_A^2}\right) \Phi_m\right] \right]^\alpha \\ \times \left\{ \int_0^{t_k} \left[ \prod_{m=0}^{k-1} \exp\left[\frac{w_l^2}{w_A^2} \exp\left(-\frac{2r^2}{w_A^2}\right) \Phi_m\right] \right]^\alpha \frac{\sigma^0 n_0}{2\sigma\tau_p} \right. \\ \left. \times \sum_{m=0}^{k-1} \Phi_m \frac{w_l^2}{w_A^2} \exp\left(-\frac{2r^2}{w_A^2}\right) \text{sech}^2\left(\frac{t - mt_r}{\tau_p}\right) dt + n_0 \right\} \quad (6) \end{aligned}$$

where  $n(r, t_k)$  and  $n^+(r, t_k)$  are the population density of the gain medium and the absorber ground-state population density at the  $k$ th roundtrip, respectively;  $n_0$  is total population density of the EL2 defect level (including EL2<sup>0</sup> and EL2<sup>+</sup>) of LT-GaAs,  $\sigma^0$  and  $\sigma^+$  are the absorption cross section of EL2<sup>0</sup> and EL2<sup>+</sup> in LT-GaAs,  $L$  is the intrinsic loss,  $R$  is the reflectivity at 1.06  $\mu\text{m}$  of the output coupler;  $B = 6\beta h\nu c(w_G/w_A)^2$  is the coupling coefficient of two-photon absorption (TPA) in LT-GaAs,  $\beta$  is the absorption coefficient of two photons;  $w_G$ ,  $w_A$ ,  $w_{ktp}$  and  $w_l$  is the radius of are the radii of TEM<sub>00</sub> mode at the positions of gain medium, LT-GaAs wafer, KTP and the average TEM<sub>00</sub> mode in the cavity, respectively, which can be calculated by ABCD matrix theory, and the calculated values are shown in Table 1.  $R_{in}(r) = P_{in} \exp(-2r^2/w_p^2) [1 - \exp(-\alpha_a l)] / h\nu_p \pi w_p^2 l$  is the pump rate, where  $P_{in}$  is the pump power,  $h\nu_p$  is the single-photon energy of the pump light,  $w_p$  is the average radius of the pump beam,  $\alpha_a$  is the absorption coefficient of the gain medium;  $\alpha = (\sigma^+ + \sigma^0) / \sigma$ ;  $n_i = [\ln(1/T_0^2 + \ln(1/R) + L) / (2\sigma l)]$  is the initial population inversion density in the gain medium,  $T_0 = \exp\{-[\sigma^0(n_0 - n^+) + \sigma^+ n^+] l_s\}$  is the small-signal transmission of LT-GaAs. With the parameters in Table 1,  $\Phi_k$  can be obtained by numerically solving equations (4–6) for a given initial value  $\Phi_0$ .

### 3.2 Nonlinear loss due to harmonic conversion

For a Q-switched intracavity-frequency-doubled laser, the second-harmonic conversion is generally considered as the nonlinear loss of the fundamental wave as introduced in references [19,21]. Under the small-signal approximation and assuming the fundamental wave as plane wave with Gaussian amplitude profile as well as ignoring the mismatch of the nonlinear crystal, the single-pass second harmonic power converted from the  $k$ th mode-locked pulse for type-II phase matching is [19,21]:

$$\begin{aligned} P_{k,2\omega}(r, t) &= \frac{K_N}{A_K} P_{k,\omega}^2(r, t) \\ &= \frac{AK_N}{8} \left( \frac{h\nu}{\sigma\tau_p} \right)^2 \frac{A}{A_K} \exp\left(-\frac{4r^2}{w_l^2}\right) \Phi_k^2 \sec^2 h^4 \left( \frac{t}{\tau_p} \right) \end{aligned} \quad (7)$$

where  $K_N = \omega^2 d_{eff}^2 d^2 / (c^3 \varepsilon_0 n_{e2}^{2\omega} n_{e2}^\omega n_{e1}^\omega)$ ,  $h\nu$  is the single photon energy of the fundamental wave,  $\omega$  is the angle frequency of fundamental wave,  $d_{eff}$  is the effective nonlinear coefficient;  $\varepsilon_0$  is the dielectric permeability of vacuum,  $n_{e2}^{2\omega}$ ,  $n_{e2}^\omega$ ,  $n_{e1}^\omega$  are the harmonic and fundamental wave refractive indices, respectively.  $A_K = (1/2)\pi w_{ktp}^2$  is the area of fundamental wave at the position of KTP;  $A = (1/2)\pi w_l^2$  is the mode area at the gain medium.

So the nonlinear loss due to harmonic conversion under Gaussian distribution can be obtained [21]:

$$\delta_k(r) = \frac{P(2\omega, r)}{P(\omega, r)} = K_N h\nu c d^2 \exp\left(-\frac{2r^2}{w_{ktp}^2}\right) \phi_{ktp}(0, t) \quad (8)$$

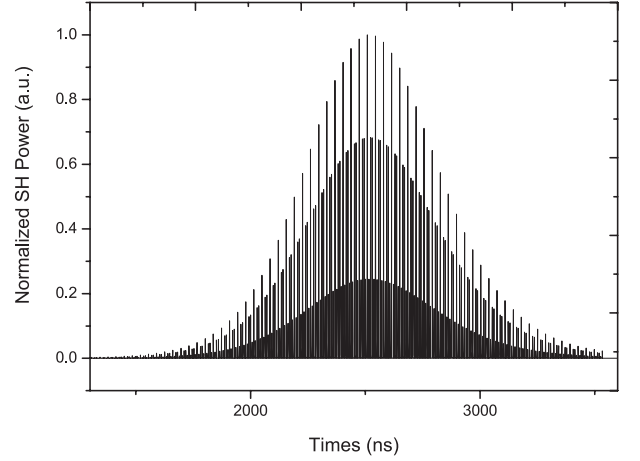


**Fig. 7.** Calculated results for the temporal shape of a single Q-switched green pulse at the pump power of 4.8 W.

where  $\phi_{ktp}(0, t)$  is the photon density in the laser axis at the position of KTP.

Then according to equations (1, 2, 7), the output second-harmonic power coupled out of the cavity can be expressed as:

$$\begin{aligned} P_{k,2\omega}(r, t) &= \frac{AK_N}{8} \left( \frac{h\nu}{\sigma\tau_p} \right)^2 \frac{A}{A_K} \\ &\times \exp\left(-\frac{4r^2}{w_l^2}\right) \sum_{k=0}^{\infty} \Phi_k^2 \sec^2 h^4 \left( \frac{t - t_k}{\tau_p} \right). \end{aligned} \quad (9)$$

By integrating equation (13) over time from zero to infinity, the output energy of the Q-switched mode-locked green pulse can be obtained as:

$$E_{2\omega} = \frac{AK_N}{6\tau_p} \frac{A}{A_K} \left( \frac{h\nu}{\sigma} \right)^2 \exp\left(-\frac{4r^2}{w_l^2}\right) \sum_{k=0}^{\infty} \Phi_k^2. \quad (10)$$

From equation (14) we can see that the total pulse energy of the Q-switched envelope of the green pulse depends on  $\tau_p$ . Using the parameters in Table 1 and equation (10), we can obtain the dependence of the total SH Q-switched pulse energy on  $\tau_p$ . Figure 8 shows such dependences at the pump power of 4.8 W. Since the duration for the mode-locked pulse at fundamental wavelength is about  $\sqrt{2}$  times of that for the SH wavelength [2], the FWHM duration  $\tau$  of mode-locked pulse at fundamental wavelength can be estimated to be 530 ps. According to the relation between  $\tau$  and  $\tau_p$ , i.e.,  $\tau = 1.76\tau_p$ . We can obtain that  $\tau_p = 300$  ps. Considering the value of  $\tau_p = 300$  ps, we also can obtain the theoretical dependence of the total pulse energy of the self-Q-switched green pulse on the incident pump power, which is shown as line in Figure 4. From Figure 4, it can be seen that the theoretical results are in good agreement with the experimental results. The calculated temporal shape of a single Q-switched green pulse at pump power of 4.8 W is shown in Figure 7, which agrees with the experimental results shown in Figure 5. From Figure 7, we

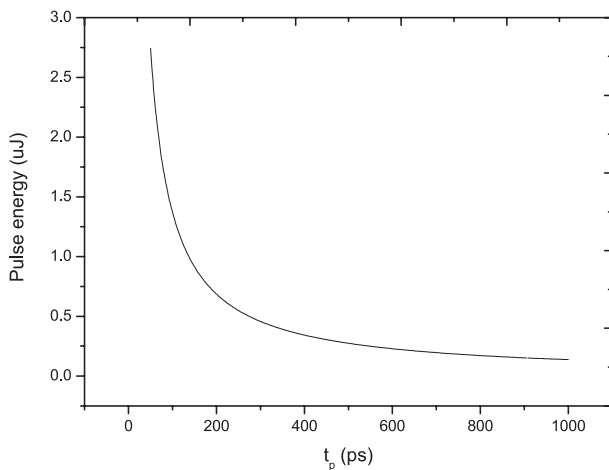


**Fig. 8.** Calculated dependence of the total energy of a single SH Q-switched envelope on  $\tau_p$  at the pump power of 4.8 W.

can see that the duration of the SH Q-switched pulse envelop is about 630 ns, which is close to the experimental results of 640 ns.

## 4 Conclusion

We have demonstrated the intracavity second harmonic generation in a passively Q-switched and mode-locked *c*-cut Nd:GdVO<sub>4</sub>/KTP green laser with LT-GaAs saturable absorber. The modulation depth for the green mode-locked pulses was more than 90% at any pump power over the threshold power. The repetition rate for the mode-locked green pulses inside the passively Q-switched pulse envelope was about 143 MHz, corresponding to one cavity roundtrip time. Based on the hyperbolic secant function methods, a rate equation model for the passively Q-switched and mode-locked laser was proposed, in which the Gaussian spatial distribution of the intracavity photon intensity, the influences of continuous pump rate, the upper state lifetime of the active medium, and the excited-state lifetime of the saturable absorber were considered. Using this theoretical model, the theoretical results are in good agreement with the experiments, and especially, the pulse width of the mode-locked green pulse was estimated to be around 380 ps.

This work was partially supported by the National Science Foundation of China (60578010 and 60678015) and the Natural Science Foundation of Shandong Province (Y2005G12).

## References

1. J.Y. Wang, Q. Zheng, Q.H. Xue, H.M. Tan, *Chin. Opt. Lett.* **1**, 604 (2003)
2. P. Mukhopadhyay, M. Alsous, K. Ranganathan, S. Sharma, P. Gupta, J. George, T. Nathan, *Appl. Phys. B* **79**, 713 (2004)
3. P. Mukhopadhyay, M. Alsous, K. Ranganathan, S. Sharma, P. Gupta, J. George, T. Nathan, *Opt. Commun.* **222**, 399 (2003)
4. Y.F. Chen, S.W. Tsai, S.C. Wang, J. Chen, *Appl. Phys. B* **73**, 115 (2001)
5. Y. Fu Chen, S.W. Tsai, S.C. Wang, *Opt. Lett.* **25**, 1442 (2000)
6. P.K. Mukhopadhyay et al., *Opt. Commun.* **222**, 399 (2003)
7. Y. Fu Chen, J. Lung Lee, H. Dau Hsieh, S. Wei Tsai, *IEEE J. Quant. Electron.* **38**, 312 (2002)
8. Y.-F. Chen et al., *Appl. Opt.* **40**, 6038 (2001)
9. J. Kong et al., *Appl. Phys. B* **79**, 203 (2004)
10. W. Yonggang, L. Chaoyang, M. Xiaoyu, Z. Zhigang, *Chin. J. Semicond.* **25**, 148 (2004)
11. Z. Zhang, L. Qian, D. Fan, X. Deng, *Appl. Phys. Lett.* **60**, 419 (1992)
12. D.Y. Shen, D.Y. Tang, K. Ueda, *Jpn J. Appl. Phys.* **41**, L1224 (2002)
13. S.P. Ng, D.Y. Tang, J. Kong, L.J. Qin, X.L. Meng, Z.J. Xiong, *Appl. Phys. B* **80**, 475 (2005)
14. C. Honninger et al., *J. Opt. Soc. Am. B* **16**, 46 (1999)
15. U. Keller, D.A.B. Miller, G.D. Boyd, T.H. Chiu, J.F. Ferguson, M.T. Asom, *Opt. Lett.* **17**, 505 (1992)
16. B. Zhang et al., *Opt. Lett.* **28**, 1829 (2003)
17. Liu Jie, Wang Yonggang, Tian Wenmiao, Gao Liyan, He Jingliang, Ma Xiaoyu, *Opt. Mat.* **28**, 970 (2006)
18. P. Kryukov, V. Letokhov, *IEEE J. Quant. Electron.* **8**, 766 (1972)
19. Kejian Yang, Shengzhi Zhao, Guiqiu Li, Ming Li, Dechun Li, Jing Wang, and Jing An, *IEEE J. Quant. Electron.* **40**, 683 (2006)
20. Kejian Yang, Shengzhi Zhao, Guiqiu Li, Ming Li, Dechun Li, Jing Wang, Jing An, *Opt. Mater.* (in press)
21. K. Yang, S. Zhao, G. Li, H. Zhao, *IEEE J. Quant. Electron.* **40**, 1252 (2004)
22. K. Yang, S. Zhao, G. Li, H. Zhao, *Jpn J. Appl. Phys.* **43**, 8053 (2004)
23. J. Liu, J. Yang, J. He, *Opt. Commun.* **219**, 317 (2003)
24. S.J. Zhang, E. Wu, H.P. Zeng, *Opt. Commun.* **231**, 365 (2004)